Refractive Index Sensing of Green Fluorescent Proteins in Living Cells Using Fluorescence Lifetime Imaging Microscopy

Henk-Jan van Manen,* Paul Verkuijlen,† Paul Wittendorp,* Vinod Subramaniam,* Timo K. van den Berg,† Dirk Roos,† and Cees Otto*

*Biophysical Engineering Group, Institute for Biomedical Technology, and MESA+ Institute for Nanotechnology, University of Twente, Enschede, The Netherlands; and †Department of Blood Cell Research, Sanquin Research, and Landsteiner Laboratory, Academic Medical Centre, University of Amsterdam, Amsterdam, The Netherlands

ABSTRACT We show that fluorescence lifetime imaging microscopy (FLIM) of green fluorescent protein (GFP) molecules in cells can be used to report on the local refractive index of intracellular GFP. We expressed GFP fusion constructs of Rac2 and gp91^{phox}, which are both subunits of the phagocyte NADPH oxidase enzyme, in human myeloid PLB-985 cells and showed by high-resolution confocal fluorescence microscopy that GFP-Rac2 and GFP-gp91^{phox} are targeted to the cytosol and to membranes, respectively. Frequency-domain FLIM experiments on these PLB-985 cells resulted in average fluorescence lifetimes of 2.70 ns for cytosolic GFP-Rac2 and 2.31 ns for membrane-bound GFP-gp91^{phox}. By comparing these lifetimes with a calibration curve obtained by measuring GFP lifetimes in PBS/glycerol mixtures of known refractive index, we found that the local refractive indices of cytosolic GFP-Rac2 and membrane-targeted GFP-gp91^{phox} are ~1.38 and ~1.46, respectively, which is in good correspondence with reported values for the cytosol and plasma membrane measured by other techniques. The ability to measure the local refractive index of proteins in living cells by FLIM may be important in revealing intracellular spatial heterogeneities within organelles such as the plasma and phagosomal membrane.

Received for publication 19 December 2007 and in final form 16 January 2008.

Address reprint requests and inquiries to Cees Otto, Tel.: 31-53-489-3159; E-mail: c.otto@utwente.nl.

Fluorescence lifetime imaging microscopy (FLIM) has become a robust technique in biochemistry and cell biology for the Förster resonance energy transfer detection of molecular interactions between protein molecules labeled with donor and acceptor members of the fluorescent protein (FP) family (1,2). Besides a sensitivity to molecular interactions (e.g., via energy transfer or collisions), fluorescence lifetimes of fluorophores are generally also dependent on other microenvironment parameters such as pH, viscosity, refractive index, and the presence of ions. Whereas viscosity has been shown not to affect the fluorescence lifetime of green fluorescent protein (GFP) (3), Suhling et al. and Borst et al. have reported that the refractive index of the microenvironment does influence the fluorescence lifetimes of GFP (4) and cyan and yellow fluorescent proteins (FPs) (5). FP lifetimes were further shown by these groups to satisfy the Strickler-Berg relationship (Eq. 1) between refractive index and fluorescence lifetime (6),

$$\frac{1}{\tau_0} = k_r = 2.88 \times 10^{-9} n^2 \frac{\int I(\tilde{\nu}) d\tilde{\nu}}{\int I(\tilde{\nu}) \tilde{\nu}^{-3} d\tilde{\nu}} \int \frac{\varepsilon(\tilde{\nu})}{\tilde{\nu}} d\tilde{\nu}, \quad (1)$$

in which τ_0 is the natural radiative lifetime (related to the fluorescence lifetime τ via the fluorescence quantum yield $\phi = \tau/\tau_0$), k_r is the radiative rate constant, n is the refractive index, I is the fluorescence emission, $\tilde{\nu}$ is the wavenumber, and ε is the extinction coefficient.

Although FLIM on FP chimeras is now one of the most suitable optical microscopy techniques to investigate molecular interactions between proteins in living cells, little is known about the effect of different intracellular refractive indices on FP fluorescence lifetimes. To investigate whether the Strickler-Berg relationship is satisfied by GFP in living cells, which would imply that FLIM can be used to sense local intracellular refractive indices, we stably expressed enhanced GFP fusion constructs of Rac2 and gp91^{phox} in human myeloid PLB-985 cells by retroviral transduction (see Supplementary Material). These cells also expressed a monomeric red FP (7) chimera of p67^{phox} which might serve as a Förster resonance energy transfer acceptor in future experiments aimed at studying the molecular interactions between gp91^{phox} or Rac2 and p67^{phox} in living cells. Gp91^{phox}, p67^{phox}, and Rac2 are all subunits of the multimeric phagocyte NADPH oxidase enzyme that plays a critical role in the innate immune response against invading microorganisms (8). Upon NADPH oxidase activation, which occurs when leukocytes ingest microorganisms by phagocytosis, oxygen is reduced by gp91^{phox} to superoxide (O_2^-). Superoxide is subsequently converted to other reactive oxygen species such as peroxide and hypochlorite, which contribute to the killing of the phagocytosed microbes. We have previously investigated (9,10) the dynamic behavior of GFP-Rac2 in resting and phagocytosing PLB-985 cells by fluorescence correlation spectroscopy and fluorescence recovery after photobleaching (FRAP) experiments, respectively. Whereas GFP-Rac2 displays a random translational diffusion in the cytosol in resting cells (10), we found that it is continuously being translocated to the phagosomal membrane in cells ingesting zymosan particles (9). At the

Editor: Egward H. Egelman.

doi: 10.1529/biophysj.107.127837

membrane of the phagosome, Rac2 has been shown to bind to membrane-embedded gp91^{phox}, which is a necessary interaction for NADPH oxidase activation to occur (11). In this study, we investigated GFP-Rac2 and GFP-gp91^{phox} by FLIM because their intracellular locations in resting cells (Rac2 is cytosolic and gp91^{phox} is membrane-bound) might give rise to different fluorescence lifetimes caused by different local refractive indices.

We first verified the subcellular localization of GFP-Rac2 in GFP-Rac2/p67^{phox}-mRFP PLB-985 cells and GFP-gp91^{phox} in PLB-985 cells by confocal fluorescence microscopy. As shown in Fig. 1 *A*, GFP-Rac2 is indeed cytosolic in resting cells. This was further confirmed by fluorescence loss in photobleaching experiments, which showed that repetitive photobleaching of a small cytosolic region causes all of the fluorescence in these cells to disappear (see Supplementary Material). As expected, confocal microscopy showed that p67^{phox}-mRFP is also cytosolic in resting GFP-Rac2/p67^{phox}-mRFP PLB-985 cells (results not shown).

As shown in Fig. 1 *C*, GFP-gp91^{phox} is mainly localized to the plasma membrane but also to intracellular vesicles of ~0.5 μm in diameter. This is consistent with reported subcellular fractionation assays on PLB-985 cells (12) and with previous microscopy studies of immunofluorescently-labeled gp91^{phox} in fixed PLB-985 cells (13) and also shows that N-terminal tagging of gp91^{phox} with GFP does not prevent the targeting of gp91^{phox} to its functional sites, i.e., the plasma membrane and vesicular membranes. In COS-7 and Chinese hamster ovary cells (which, in contrast to PLB-985 cells differentiated into neutrophil-like cells, are nonphagocytic cells), GFP-gp91^{phox} has also been reported to localize in the plasma membrane and intracellular membranes (14).

We next performed frequency-domain FLIM experiments on resting GFP-gp91^{phox}, GFP-gp91^{phox}/p67^{phox}-mRFP, and GFP-Rac2/p67^{phox}-mRFP PLB-985 cells using a wide-field fluorescence microscope equipped with a Lambert Instruments Fluorescence Attachment for lifetime imaging (see Supplementary Material). A blue light-emitting diode (λ_{max} = 468 nm) modulated at 40 MHz was used to excite GFP. Fluorescence detection was performed by a combination of a modulated (40 MHz) image intensifier and a charge-coupled device camera, providing a spatial resolution of ~0.35 μm/pixel in FLIM images. A narrow emission bandpass filter (520/35 nm) was used to allow detection of GFP only and suppress any fluorescence emission from mRFP attached to p67^{phox}. FLIM measurements were calibrated by a 10-μM solution of rhodamine 6G, the lifetime of which was set to 4.11 ns (15). Fig. 2, *B* and *D*, show representative FLIM images of resting GFP-gp91^{phox} and GFP-Rac2/p67^{phox}-mRFP cells, respectively.

It is clear from these images that the average lifetime of membrane-bound GFP-gp91^{phox} is significantly reduced compared to cytosolic GFP-Rac2 in PLB-985 cells. By averaging FLIM data of many cells, the fluorescence lifetime histograms shown in Fig. 3 were obtained. The highly overlapping blue and green histograms indicate that the presence of p67^{phox}-mRFP does not influence the lifetime of GFP-gp91^{phox} in GFP-gp91^{phox}/p67^{phox}-mRFP cells. We therefore also assume that the red curve in Fig. 3 is representative for GFP-Rac2 only, despite the presence of p67^{phox}-mRFP in these cells. Gaussian fitting of the histograms in Fig. 3 resulted in average lifetimes of 2.31 ± 0.25 ns and 2.70 ± 0.20 ns for GFP-gp91^{phox} and GFP-Rac2, respectively. To relate the observed fluorescence

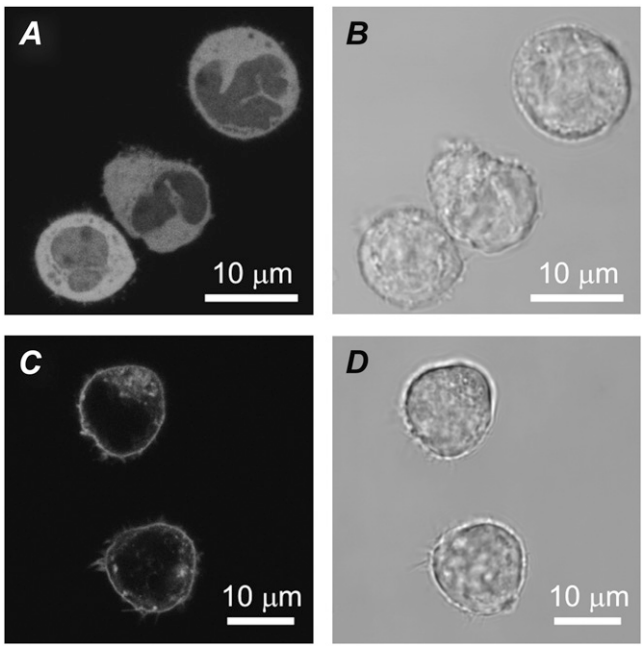

FIGURE 1 Confocal fluorescence images (*A* and *C*) of GFP-Rac2/p67^{phox}-mRFP (*A*) and GFP-gp91^{phox} (*C*) PLB-985 cells. Corresponding bright-field images are shown in *B* and *D*.

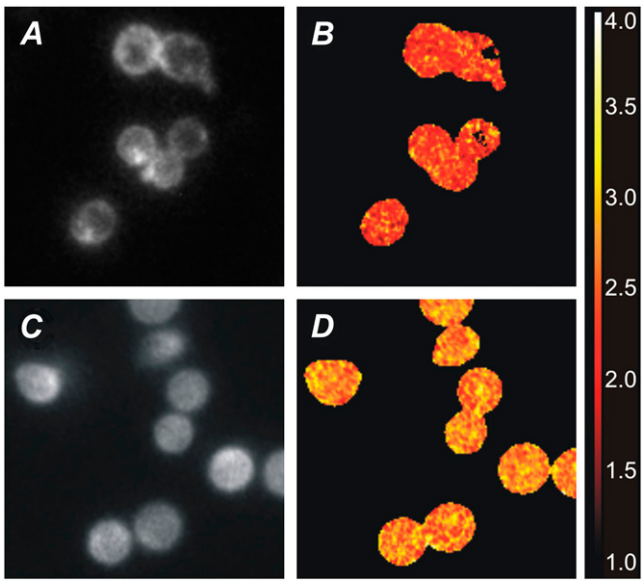

FIGURE 2 Fluorescence intensity (*A* and *C*) and FLIM (*B* and *D*) images of GFP-gp91^{phox} (*A* and *B*) and GFP-Rac2/p67^{phox}-mRFP (*C* and *D*) PLB-985 cells. The lifetime scale bar ranges from 1 to 4 ns.

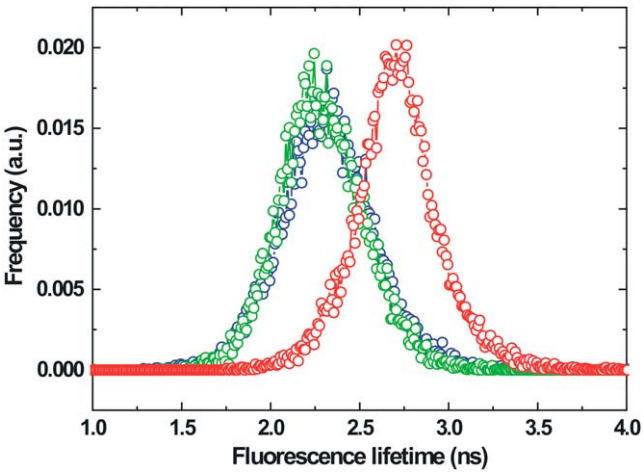

FIGURE 3 Fluorescence lifetime histograms of GFP-gp91^{phox} (*blue*), GFP-gp91^{phox}/p67^{phox}-mRFP (*green*), and GFP-Rac2/p67^{phox}-mRFP (*red*) PLB-985 cells. Curves represent FLIM data recorded from 32 (*blue*), 28 (*green*), and 65 (*red*) cells.

lifetimes of the different GFP chimeras in PLB-985 cells to different refractive indices, we constructed a calibration curve by measuring the fluorescence lifetime of GFP in PBS/glycerol mixtures of varying refractive index (see Supplementary Material), in analogy with a previous study (4). Using this calibration curve, the lifetimes for GFP-Rac2 in the cytosol and GFP-gp91^{phox} in membranes correspond to local refractive indices of 1.38 ± 0.04 and 1.46 ± 0.06, respectively. These values closely resemble recently reported refractive indices for the cytosol, e.g., $n = 1.36$ (16) and $n = 1.36-1.39$ (17), and previous estimates for the plasma membrane, e.g., $n = 1.46-1.60$ (18) using phase microscopy techniques. Interestingly, in FLIM experiments using GFP physisorbed to polystyrene microspheres ($n = 1.59$), we found that the average fluorescence lifetime of GFP close to the PS surface is ~1.84 ns (results not shown), which according to our GFP calibration curve corresponds to a local refractive index of 1.60. These experiments therefore validate our FLIM results on GFP chimeras in PLB-985 cells.

In conclusion, we have demonstrated that FLIM enables the local refractive index of GFP chimeras in living cells to be measured. FLIM may therefore be valuable in studies aimed at investigating local heterogeneities in cellular structures such as membranes (19).

SUPPLEMENTARY MATERIAL

To view all of the supplemental files associated with this article, visit www.biophysj.org.

ACKNOWLEDGMENTS

Financial support from the Landsteiner Foundation for Blood Transfusion Research (Amsterdam, The Netherlands) is gratefully acknowledged. We thank Dr. Lydia Henderson (University of Bristol, UK) for the GFP-gp91^{phox} vector. H.-J.v.M. thanks Dr. Thomas Jovin and Dr. Donna Arndt-Jovin for their hospitality and for stimulating FLIM discussions during a three-months visit to their laboratory at the Max Planck Institute for Biophysical Chemistry (Göttingen, Germany), which was financially supported (short-term fellowship ASTF No. 259-2005 to H.-J.v.M.) by the European Molecular Biology Organization (Heidelberg, Germany).

REFERENCES and FOOTNOTES

1. Festy, F., S. M. Ameer-Beg, T. Ng, and K. Suhling. 2007. Imaging proteins *in vivo* using fluorescence lifetime microscopy. *Mol. Biosyst.* 3:381–391.
2. Van Munster, E. B., and T. W. J. Gadella. 2005. Fluorescence lifetime imaging microscopy. *Adv. Biochem. Eng. Biotechnol.* 95:143–175.
3. Suhling, K., D. M. Davis, and D. Phillips. 2002. The influence of solvent viscosity on the fluorescence decay and time-resolved anisotropy of green fluorescent protein. *J. Fluoresc.* 12:91–95.
4. Suhling, K., J. Siegel, D. Phillips, P. M. W. French, S. Lévêque-Fort, S. E. D. Webb, and D. M. Davis. 2002. Imaging the environment of green fluorescent protein. *Biophys. J.* 83:3589–3595.
5. Borst, J. W., M. A. Hink, A. van Hoek, and A. J. W. G. Visser. 2005. Effects of refractive index and viscosity on fluorescence and anisotropy decays of enhanced cyan and yellow fluorescent proteins. *J. Fluoresc.* 15:153–160.
6. Strickler, S. J., and R. A. Berg. 1962. Relationship between absorption intensity and fluorescence lifetime of molecules. *J. Chem. Phys.* 37:814–882.
7. Campbell, R. E., O. Tour, A. E. Palmer, P. A. Steinbach, G. S. Baird, D. A. Zacharias, and R. Y. Tsien. 2002. A monomeric red fluorescent protein. *Proc. Natl. Acad. Sci. USA.* 99:7877–7882.
8. Cross, A. R., and A. W. Segal. 2004. The NADPH oxidase of professional phagocytes—prototype of the NOX electron transport chain systems. *Biochim. Biophys. Acta.* 1657:1–22.
9. Van Bruggen, R., E. Anthony, M. Fernandez-Borja, and D. Roos. 2004. Continuous translocation of Rac2 and the NADPH oxidase component p67^{phox} during phagocytosis. *J. Biol. Chem.* 279:9097–9102.
10. Van Manen, H.-J., R. Van Bruggen, D. Roos, and C. Otto. 2006. Single-cell optical imaging of the phagocyte NADPH oxidase. *Antioxid. Redox Signal.* 8:1509–1522.
11. Bokoch, G. M., and T. Zhao. 2006. Regulation of the phagocyte NADPH oxidase by Rac GTPase. *Antioxid. Redox Signal.* 8:1533–1548.
12. Yu, L., F. R. DeLeo, K. J. Biberstine-Kinkade, J. Renee, W. M. Nauseef, and M. C. Dinauer. 1999. Biosynthesis of flavocytochrome b_{558}. Gp91^{phox} is synthesized as a 65-kDa precursor (p65) in the endoplasmic reticulum. *J. Biol. Chem.* 274:4364–4369.
13. Zhen, L., L. Yu, and M. C. Dinauer. 1998. Probing the role of the carboxyl terminus of the gp91^{phox} subunit of neutrophil flavocytochrome b_{558} using site-directed mutagenesis. *J. Biol. Chem.* 273:6575–6581.
14. Murillo, I., and L. M. Henderson. 2005. Expression of gp91^{phox}/Nox2 in COS-7 cells: cellular localization of the protein and the detection of outward proton currents. *Biochem. J.* 385:649–657.
15. Hanley, Q. S., V. Subramaniam, D. J. Arndt-Jovin, and T. M. Jovin. 2001. Fluorescence lifetime imaging: multi-point calibration, minimum resolvable differences, and artifact suppression. *Cytometry.* 43:248–260.
16. Curl, C. L., C. J. Bellair, T. Harris, B. E. Allman, P. J. Harris, A. G. Stewart, A. Roberts, K. A. Nugent, and L. M. D. Delbridge. 2005. Refractive index measurements in viable cells using quantitative phase-amplitude microscopy and confocal microscopy. *Cytometry A.* 65:88–92.
17. Choi, W., C. Fang-Yen, K. Badizadegan, S. Oh, N. Lue, R. R. Dasari, and M. S. Feld. 2007. Tomographic phase microscopy. *Nat. Methods.* 4:717–719.
18. Beuthan, J., O. Minet, J. Helfmann, M. Herrig, and G. Müller. 1996. The spatial variation of the refractive index in biological cells. *Phys. Med. Biol.* 41:369–382.
19. Treanor, B., P. M. P. Lanigan, S. Kumar, C. Dunsby, I. Munro, E. Auksorius, F. J. Culley, M. A. Purbhoo, D. Phillips, M. A. A. Neil, D. N. Burshtyn, P. M. W. French, and D. M. Davis. 2006. Microclusters of inhibitory killer immunoglobulin-like receptor signaling at natural killer cell immunological synapses. *J. Cell Biol.* 174:153–161.